Morphology and Properties of Nanocomposites from Organoclays with Reduced Cation Exchange Capacity

F. Chavarria,[1] K. Nairn,[2] P. White,[2] A. J. Hill,[2] D. L. Hunter,[3] D. R. Paul[1]

[1]*The University of Texas at Austin and Texas Materials Institute, The University of Texas at Austin, Austin, Texas 78712*
[2]*CSIRO Manufacturing Science and Technology, Private Bag 33, Clayton South, MDC, Victoria 3169, Australia*
[3]*Southern Clay Products, Inc., 1212 Church Street, Gonzales, Texas 78629*

Received 26 November 2006; accepted 24 January 2007
DOI 10.1002/app.26362
Published online 16 May 2007 in Wiley InterScience (www.interscience.wiley.com).

ABSTRACT: Organoclays with different levels of reduction in the original cation exchange capacity (CEC) were prepared to characterize the morphology and Young's modulus of their melt-processed nanocomposites made from nylon 6 (PA-6) and polypropylene/polypropylene grafted with maleic anhydride (PP/PP-*g*-MA). Wide-angle X-ray scattering (WAXS), transmission electron microscopy (TEM), and Young's modulus data are reported. Three different levels of CEC reduction were obtained; WAXS analysis and percentage loss on ignition (LOI) calculations for these organoclays showed a reduction in both the intergallery spacing and in the amount of organic modifier contained in the clay with CEC reduction. The morphology and modulus results show that these reduced-CEC organoclays led to lower exfoliation and modulus enhancement for both PA-6 and PP/PP-*g*-MA nanocomposites. The results may be influenced by differences in layer charge and charge distribution that could have been produced during the charge reduction process. © 2007 Wiley Periodicals, Inc. J Appl Polym Sci 105: 2910–2924, 2007

Key words: nanocomposites; cation exchange capacity; organoclays

INTRODUCTION

Research on polymer nanocomposites formed from organoclays has been intense over the last few years as a result of the potentially superior properties that these materials can exhibit compared to conventional composites. Numerous studies have shown that the addition of a very low percentage of layered silicates can lead to a significant enhancement in many properties, such as stiffness and strength,[1–3] flame retardancy,[4,5] gas barrier properties,[6] ionic conductivity,[7,8] thermal stability,[9] and tunable biodegradability.[4] All these properties make these materials interesting prospects for a wide variety of applications, e.g., automotive, electronics, food packaging, biotechnology, and others.

High levels of exfoliation require favorable polymer–organoclay interactions and optimum processing conditions. Under the best possible processing conditions, the affinity of the polymer for the polar clay surface and/or for the nonpolar organic modifier is very important for obtaining high clay platelet dispersion and mechanical property enhancement. Processing conditions aid in reducing clay particle size and in ensuring good contact between the polymer and the organoclay, but good chemistry is required to produce exfoliation.[10] Previous studies from our laboratories have shown that the best clay dispersion and mechanical property enhancement for nylon 6 (PA-6) nanocomposites is obtained when using an organoclay formed from a surfactant with one alkyl tail, i.e., a one-tailed organoclay, that permits some access of the polymer chains to the silicate surface. On the other hand, the opposite is observed for nanocomposites made from polypropylene/polypropylene grafted with maleic anhydride (PP/PP-*g*-MA) systems and various polyethylene copolymers, i.e., higher clay dispersion and mechanical property enhancement are observed when using organic modifiers with more than one tail that provide a higher coverage of the polar clay surface and, therefore, less access of the polymer to the silicate surface.[11–13] An independent way to assess the effect of surface coverage of the clay by the surfactant on morphology and properties of nanocomposites is to reduce the cation exchange capacity (CEC) of the clay. A smaller number of exchangeable cations in the clay will reduce the amount of alkyl ammonium ions that can be exchanged onto the silicate surface and, hence, reduce the degree of organoclay surface coverage by the surfactant.

It is widely known that the layer charge of smectites can be reduced by a process known as the Hoffman–Klemen effect, where heating lithium-montmorillonite

Correspondence to: D. R. Paul (drp@che.utexas.edu).
Contract grant sponsor: Consejo Nacional de Ciencia y Tecnología (CONACyT) of Mexico.

TABLE I
Polymer and Organoclay Materials Used in This Work

Material (designation used here)	Supplier designation	Specifications	Supplier
Nylon 6 (PA-6)	Capron B135WP	M_n = 29,300[a]; MFI = 1.2 g/10 min	Honeywell
Polypropylene (PP)	Hi-Fax PH020	MFI = 37 g/10min (230°C)	Basell
Maleated polypropylene (PP-*g*-MA)	Polybond 3200	wt % MA = 1.0	Uniroyal Chemical Co.
$M_3(HT)_1$	SPX 1137: Trimethyl hydrogenated-tallow ammonium chloride organoclay	95 MER[b]; Organic content = 29.6 wt %; d_{001} spacing = 18.0 Å	SCP[c]
$M_2(HT)_2$	Cloisite 20A: Dimethyl bis(hydrogenated-tallow) ammonium chloride organoclay	95 MER; Organic content = 39.6 wt %; d_{001} spacing = 24.2 Å	SCP

[a] M_n determined via intrinsic viscosity using *m*-cresol at 25°C.
[b] MER: Milliequivalent ratio [mequiv/100 g of clay].
[c] Southern Clay Products (SCP), Gonzales, TX.

(Li-MMT) at temperatures between 200 and 300°C causes the transition of exchangeable lithium (Li^+) ions to a nonexchangeable state. Lithium fixation is produced by the partial migration of Li^+ ions from the clay galleries into the silicate layers reducing the total layer charge.[14] The extent of Li^+ fixation depends on the type of smectite, the temperature of heating, and its duration.[15–19] Alternatively, different levels of charge reduction can be obtained at the same temperature in bi-ionic lithium–sodium montmorillonites (Li–Na-MMTs) by varying the amount of exchangeable Li^+ and Na^+ ions prior to heating the clay samples.[20] The smaller size of the Li^+ ions allows them to migrate into the MMT layers, where they are not available for exchange, while the larger Na^+ ions mainly stay within the gallery and are exchangeable.

Layer charge reduction produces a decrease in the clay basal spacings, as well as in the solvation and swelling ability of the clay.[16–25] Calvet and Prost showed that the limiting value of exchangeable cations necessary to expand previously-heated montmorillonite in water was 50%, since water molecules cannot reach the internal surface when this value is lower.[16] Similar conclusions were reached by Brindley and Ertem, where they state that full expansion in water ceases when the exchangeable cations fall below 60 mequiv/100 g of clay.[20] Komadel et al. and Hrobarikova et al. show that the swelling ability of lithium–calcium montmorillonite (Li–Ca-MMT) is considerably reduced after heating at temperatures above 150°C.[18,19] Some authors suggest that this might be due to the collapse of interlayers from heterogeneous charge distribution in pristine MMT as well as the nonhomogeneous charge reduction that can be produced by ion segregation in bi-ionic montmorillonites.[22–25]

To our knowledge, the effect of charge reduction on the morphology and mechanical properties of melt-processed nanocomposites has not been studied. The one report on reduced-CEC polymer nanocomposites was based on the formation of thin-film composites in a polyimide matrix by chemical methods.[26] The object of this study is to explore the effect of CEC reduction on the morphology and Young's modulus of PA-6 and PP/PP-*g*-MA organoclay nanocomposites prepared by melt processing. Considering the arguments about the affinity of the polymer for the silicate surface versus the optimal number of alkyl tails on the surfactant mentioned above, it might be expected that a lower CEC may aid in the exfoliation of nanocomposites made with PA-6 while this most likely would reduce the degree of exfoliation that could be achieved in PP/PP-*g*-MA nanocomposites.

EXPERIMENTAL

Materials

A brief description of the materials used in this study is given in Table I. An extrusion grade of PA-6 and different PP/PP-*g*-MA blends were melt-processed with reduced-CEC organoclays to form nanocomposites. The PA-6 and the PP/PP-*g*-MA system used here were chosen based on previous studies performed in our laboratory, which showed high platelet dispersion and mechanical property enhancement of their nanocomposites.[12,27,28] The relative amounts of PP and PP-*g*-MA contained in the nanocomposites were established to have a 1 : 1 ratio of PP-*g*-MA to organoclay. All data are reported in terms of weight percent montmorillonite (wt % MMT) in the composite rather than the amount of organoclay since the silicate is the reinforcing component.

Melt processing

PA-6 and PP/PP-*g*-MA nanocomposites were formed in a 5 mL DSM microcompounder that consists of a vertical barrel with two conical screws (screw diameter ranges from 0.43 to 1 cm, screw length = 10.75 cm), as described previously.[29] A screw speed of 100 rpm and a residence time of 10 min were used, while each 3 g batch produced in the DSM microcompounder was injection molded into bars (7.3 × 1 × 0.32 cm) using a DSM bench-top microinjection molder. PA-6 nanocomposites were formed using a barrel temperature of 240°C, an injection molder cylinder temperature of 260°C, and a mold temperature of 80°C, while PP/PP-*g*-MA nanocomposites were formed using a barrel temperature of 185°C, an injection molder cylinder temperature of 210°C, and a mold temperature of 40°C. The injection pressures were 4 and 3 bar for PA-6 and PP/PP-*g*-MA nanocomposites, respectively. After molding, the specimens were sealed and placed in a vacuum desiccator for a minimum of 24 h prior to mechanical testing.

Testing and characterization

The amount of MMT in each composite was determined by heating the predried nanocomposites in a furnace at 900°C for 45 min. Values of wt % MMT were calculated by weighing the residual ash and correcting for the loss of structural OH groups in the form of water (dehydroxylation), using the following equation:[27,30]

$$\%\mathrm{MMT} = \%\mathrm{MMT}_{\mathrm{ash}}/0.935 \quad (1)$$

where % $\mathrm{MMT}_{\mathrm{ash}}$ is the mass after incineration, relative to the original nanocomposite mass.

The percentage loss on ignition (LOI) is obtained by the same heating procedure using dry organoclay in powder form; this gives the amount of organic modifier contained within the galleries of the pristine organoclay.

CEC determination was performed on dry montmorillonite clays by saturating the exchange sites with ammonium ions followed by the extraction and titration of the exchanged ammonium. This is done by two cation exchange reactions: in the first one, the surface and intergallery cations of the MMT are exchanged with ammonium ions by reacting the clay with ammonium acetate, the remaining clay is then purified with ethanol, and pure ammonium-MMT is obtained. In the second cation exchange reaction, the ammonium-MMT is reacted with sodium hydroxide to extract the ammonium ions; the extracted solution is heated to produce ammonia, which is distilled, into an excess of boric acid. Hydrochloric acid is then used to titrate the ammonium borate and measure the amount of exchangeable cations in the clay, i.e., the CEC of the clay.

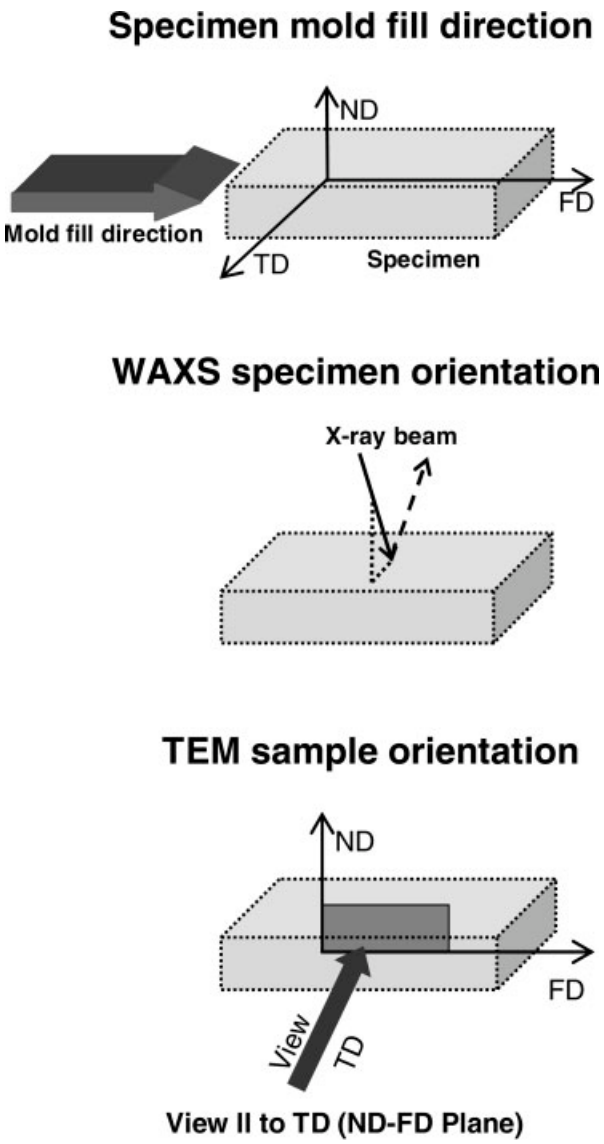

Figure 1 Specimen mold fill direction, WAXS specimen orientation, and TEM sample orientation used in this work.

The stiffness of the composites was characterized by the Young's modulus from the tensile samples obtained by testing a total of three specimens five times each and averaging the responses; these five repetitions were performed under 1% strain where no hysteresis could be detected.[29,31] Standard deviations were typically of the order of 1–10% for the samples based on PA-6, and 1–4% for the samples based on PP/PP-*g*-MA.

Wide-angle X-ray scattering (WAXS) scans were obtained using a Scintag XDS 2000 diffractometer in reflection mode, with an incident wavelength of 1.542 Å at a scan rate of 1.0 deg/min. These analyses were performed using tensile bars for the polymer samples while the clay was analyzed in powder form.

TABLE II
Details for Li–Na-MMTs

Clay (designation used here)	Composition	Target Li^+:Na^+ ratio	Amount of LiCl added	Heating treatments
A	Li–Na-MMT	1 : 3	2.0 g (47.2 mmol)	48 h at 150°C
B	Li–Na-MMT	2 : 3	3.9 g (92.0 mmol)	48 h at 150°C
C	Li–Na-MMT	3 : 3	5.9 g (139.2 mmol)	48 h at 150°C

Transmission electron microscopy (TEM) images were obtained using a Phillips EM208 transmission electron microscope with an accelerating voltage of 80 kV. Samples for TEM were cryogenically cut into ultrathin sections (50–70 nm thick), with a diamond knife at temperatures of −40 and −60°C for PA-6 and PP/PP-*g*-MA nanocomposites, respectively, using an RMC PowerTome XL ultramicrotome with a CR-X universal cryosectioning system. These sections were taken from the central part of the injection molded bar normal to the transverse direction (TD) and viewed in the TEM parallel to the transverse direction, as shown in Figure 1.

CEC reduction of sodium montmorillonite

Three reduced-CEC montmorillonite clays, i.e., clays A, B, and C, were prepared by exchanging specific percentages of the Na^+ ions contained in sodium montmorillonite with Li^+ ions through a cation exchange reaction between sodium montmorillonite and lithium chloride (LiCl), followed by heating at 150°C for 48 h to induce Li^+ fixation. The initial amounts of LiCl for each sample were calculated considering that 1 g of clay contained approximately 1 mmol of exchangeable Na^+ and were targeted to have 1 : 3, 2 : 3, and 1 : 1 ratios of Li^+ to Na^+ ions in the exchange reaction. The cation exchange reactions were performed by dissolving the LiCl in 3 L of filtered deionized water (milli-Q water) and adding 150 g of sodium montmorillonite. The mixture was stirred for 48 h and later centrifuged in a Spintron GT-155 centrifuge at 2000 rpm for 6 h. After this, 200 mL of the supernatant were decanted and the remaining mixture was resuspended by shaking with an additional 400 mL of milli-Q water. The suspension was again centrifuged while keeping the contents refrigerated to promote the separation of the clay from solution. A second supernatant was decanted and the remaining suspension was washed several times to remove any excess Li^+, Na^+, and/or Cl^- ions. The residual slurry was oven dried for 16 h; the temperature was then increased to 150°C for 48 h to induce Li^+ fixation and obtain layer charge reduction. Table II shows details for the clays as well as the initial amounts of LiCl added for each clay.

Table III shows inductively coupled plasma (ICP) analyses of Li^+ and Na^+ concentrations from the two supernatants extracted after the cation exchange reaction. This table shows that the solvation of Na-MMT leaches a high concentration of Na^+ ions into solution. The supernatants extracted from the clay solutions containing Li^+ ions show a higher concentration of Na^+ ions than the one observed from the solvation of Na-MMT, and this concentration increases as the initial lithium concentration is increased. These results also show that the Li^+ concentration in the first supernatant from clay A is lower than the corresponding standard lithium solution, which suggests that a portion of the Li^+ ions are removed from solution after the cation exchange reaction. Further analyses of the results were not performed due to problems with separating the clay from the supernatant and, hence, it was very difficult to estimate the exact amount of clay remaining after the extractions. X-ray results before and after the heating of clay C show a slight decrease in *d*-spacing from 1.26 to 1.23 nm after heating at 150°C for 48 h.

CEC measurements for these clays suggest that only a minor CEC reduction was obtained (between 4% and 7%) and that the CEC values were very similar for all three clays, i.e., 88, 85, and 88 meqiv/100 g of clay

TABLE III
ICP Analysis Results[a]

Sample	Lithium (ppm)	Sodium (ppm)
Milli-Q water-background	< 0.2	< 5.0
Li^+ Standard solution (Li^+ concentration equivalent to B)	83	< 5.0
Na-MMT—supernatant (solvation of Na-MMT)	< 0.2	425
Clay A		
1st supernatant	45	677
2nd supernatant	33	505
Clay B		
1st supernatant	102	775
2nd supernatant	67	512
Clay C		
1st supernatant	179	884
2nd supernatant	93	445

[a] Approximately 2 mL of supernatant was taken for each measurement, and these samples were prefiltered through a 0.45 μm syringe filter prior to analysis.

TABLE IV
Composition and Heating Treatments Performed for the Reduced-CEC Clays Used to Form Organoclays

Clay (designation used here)	Composition	Heating treatments	Charge reduction
Control	Na-MMT	None	None
D	Clay B	(a) 1 h at 80°C (b) 2 h at 300°C	Low
E	Clay A	(a) 24 h at 150°C (b) 24 h at 300°C	Medium
F	Clay C	(a) 24 h at 150°C (b) 24 h at 300°C	High

for clays A, B, and C, respectively. For this reason, subsequent heating trials were performed, to determine if a higher CEC reduction could be achieved by increasing the temperature and duration of heating. The heating trials performed show that heating a sample of clay B for another 48 h at 150°C led to no significant change in CEC; similarly, heating a sample of clay A for 2 h at 250°C produced almost no change in CEC either. The lowest CEC values obtained for each clay in these trials were 77, 73, and 65 mequiv/100 g of clay for clays A, B, and C, respectively, by heating for 24 h at 250°C. The results also show that heating another sample of clay C for 36 h at 300°C led to the same CEC reduction as when heating at 250°C for 24 h. These values correspond to CEC reductions of approximately 16%, 21%, and 30%, respectively, which are lower than what was targeted by exchanging 25%, 40%, and 50% of the Na^+ ions by Li^+ ions in Na-MMT. It is important to add that all the aforementioned samples showed good dispersion in water and that WAXS scans from these samples at 50% relative humidity and of glycolated films showed the typical d_{001} spacings for Na-MMT, i.e., 1.2 and 1.7 nm, respectively.[32]

Based on the results obtained from the heating trials, the CEC in these clays could not be lowered past a certain value even after heating at high temperatures for up to 36 h. Reports in the literature show that heating Li–Na-MMT clays at a temperature of 220°C for 24 h can lead to reductions in CEC of over 60%.[16,21,22] Possible reasons for not reaching lower CECs could be (1) the incomplete exchange of Li^+ for Na^+ ions during the cation exchange, (2) the Li^+ ions did not effectively migrate inside the clay galleries remaining mostly at the clay surface, and/or (3) the extent of Li^+ fixation into the clay layers during heating was lower than the expected. Some authors suggest that the presence of other ions such as Ca^+ or Na^+ may inhibit Li^+ fixation upon heating,[19] and that variations in charge location due to heterogeneity in the charge density of the pristine clay[24,25] may also affect CEC reduction.

Even though the CEC reduction was not as high as expected, subsequent heating was performed on these clays to have three different levels of CEC reduction, i.e., a low, an intermediate, and the highest achievable CEC reduction. Since the measurements following the heating trials showed very similar CEC values for clays A and B, clay B was heated at 80°C for 1 h with the aim of achieving the lowest level of CEC reduction (clay D) and clay A was heated at 250°C for 24 h to obtain an intermediate CEC reduction (clay E). Additionally, clay C was heated at 250°C for 24 h with the aim of achieving the highest level of CEC reduction (clay F). Preliminary CEC measurements on the twice-heated clays showed that the reduction in CEC was still low in all three clays. For this reason, a third heating treatment was performed to make sure the CEC was reduced; clays E and F were heated at 300°C for an additional 24 h, while clay D was heated at the same temperature for 2 h. A summary of the heating treatments performed on each clay is described in Table IV. Further CEC measurements were not performed due to the small amounts of reduced-CEC clays that were obtained; however, the layer charge will be estimated for each clay from the number of equivalents of surfactant contained in the organoclays prepared from them, by calculating the percentages of MMT and organic from LOI measurements.

Two different types of organoclays based on $M_3(HT)_1$ and $M_2(HT)_2$ surfactants were produced from each reduced-CEC clay, i.e., clays D, E, and F; control samples for each type of organoclay with no CEC reduction were also made from Na-MMT for comparison. The organoclays were formed by dispersing the clays in water and mixing at high velocities to form slurries with concentrations of 1% solids. The slurries were later heated to 80°C and mechanically stirred. Chloride salts of the corresponding quaternary ammonium surfactants were added to each clay and the solutions were left to react for 1.5 h. The reaction products were vacuum-filtered, washed with methanol to remove the excess surfactant, and then washed with distilled water to remove the remaining methanol. The wet clays were oven dried at 60°C for 16 h, and then milled to produce organoclay powders. The amount of alkyl ammonium chloride in each reaction

TABLE V
LOI Percentage and Layer Charge Estimations for the Organoclays Used in This Study

		Surfactant					
		$M_2(HT)_2$			$M_3(HT)_1$		
Clay	Charge reduction of clay	LOI (%)	Organic content (%)	Equivalents of surfactant[a] (mequiv/100 g of clay)	LOI (%)	Organic content (%)	Equivalents of surfactant[b] (mequiv/100 g of clay)
Control	None	37.8	33.4	95.1	25.1	19.9	82.3
D	Low	34.2	29.6	79.8	23.9	18.6	76.1
E	Med	33.0	28.4	75.0	24.1	18.9	77.5
F	High	30.3	25.5	64.8	21.2	15.7	61.8
Commercial organoclays							
Cloisite 20A	None	38[c]	33.7	96.2			
SPX 1137	None				28[c]	23	99.2
Control(NP)[d]	None	38.8	34.5	99.8	26.8	21.7	92.1

[a] $MW_{M\ (HT)_2} = 528$ g/mol.
[b] $MW_{M_3(HT)_1} = 301$ g/mol.
[c] Values reported by SCP.
[d] LOI and estimated layer charge results prior to purification of organoclays. Layer charge ≈ Equivalents of surfactant = % organic*(1000/MW_{surf}) × (100/% MMT); % organic = 100 – % MMT, % MMT = (100 – LOI)/0.935.

was kept constant to have 95 meqiv of surfactant/100 g of clay (an MER of 95), which is the amount used for the preparation of the commercial organoclays that will also be used for comparison, i.e., Cloisite 20A and SPX 1137 described in Table I.

Table V shows the percent LOI obtained for the organoclays described above, along with the percent of organic and the number of equivalents of surfactant calculated from the LOI values. These results show that the organoclays containing a surfactant with two long alkyl tails have a higher organic content than the organoclays that have a surfactant with only one long alkyl tail as expected. Also, for both types of organoclays, the organic content of the control is higher than those of the organoclays with a reduced-CEC; the surfactant content more or less decreases in proportion to the CEC reduction. The organoclays with low and medium CEC reductions show a very similar organic content, while the organoclays with the highest CEC reduction show the lowest. In addition, the organic contents obtained for the commercial organoclays are higher than those for the control organoclays for both cases.

In the commercial production of organoclays, the milliequivalent exchange ratio of 95 mequiv/100 g of clay used for these organoclays is slightly higher than the reported CEC for this montmorillonite, i.e., 92 mequiv/100 g of clay. This is done to ensure a reaction yield higher than 98%. Taking this into account, the percentage of organic in a fully exchanged organoclay with no CEC reduction should be around 33% (±0.5%) for $M_2(HT)_2$ and around 22% (±0.5%) for $M_3(HT)_1$. Table V shows that the percent of organic calculated for the control organoclays is within the estimated range for the two-tailed control organoclay, while it is slightly lower for the organoclay containing the one-tailed organic modifier. The percentages of organic obtained for the reduced-CEC organoclays are well below the estimated range for both types of organoclays and different percentages of organic can be observed with varying CEC reduction. For both types of organic surfactants, the percent of organic calculated for the commercial organoclays is slightly higher than the value obtained for the control organoclays, yet very close to the estimated range of percent of organic for a fully exchanged organoclay.

The main differences between the commercial and control organoclays stem from the differences in the conditions of the cation exchange reaction, e.g., the concentration of solids in the clay slurry before addition of the alkyl ammonium surfactant, and from the purification procedure performed for the control and reduced-CEC organoclays to remove the excess surfactant contained in the clay galleries. LOI measurements performed for the control organoclays prior to purification (also in Table V) show that in the case of the two-tailed surfactant, the organic content before purification is slightly higher than that estimated for the two-tailed commercial organoclay, while a slightly lower value was obtained in the case of the one-tailed organic modifier with respect to the one-tailed commercial organoclay. In addition, the organic content in the control organoclays before purification is higher than that after purification for both types of organic modifiers. Xie et al. report a decrease in organic content for commercial $M_2(HT)_2$ organoclays after washing three times with methanol.[33] They also mention that organoclays formed using an MER higher than 95 showed a larger decrease in organic content than those formed using an MER of 95 after washing with metha-

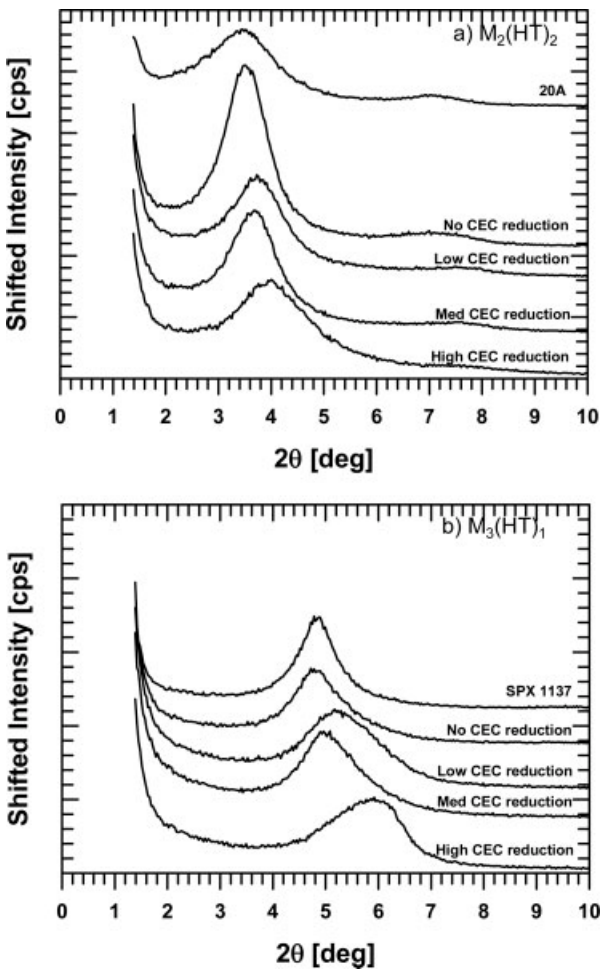

Figure 2 WAXS scans for the organoclays used in this study.

nol; in both cases, the organic content after washing was slightly lower than the expected value of 33%. The slightly lower organic content observed here for the control organoclay with the one-tailed organic modifier may imply that the yield of the cation exchange reaction with the alkyl ammonium surfactant was lower than expected, or that the washing procedure introduced a fraction of acidic protons that may have reduced the effective CEC of the aluminosilicates.[33]

The number of equivalents of surfactant calculated by dividing the mass of organic modifier inside the clay galleries by its molecular weight provides an estimate of the average clay layer charge; that is, assuming a high enough alkyl ammonium exchange yield, the number of equivalents of surfactant should be close to the clay layer charge. The results of this calculation are also shown in Table V. It can be seen that the estimated clay layer charge obtained from the reduced-CEC organoclays is lower than that obtained from the control organoclays, which in turn is lower than the values obtained from the commercial organoclays. These values are similar for each reduced-CEC clay, i.e., clays D, E, and F, and are independent of the surfactant used. The values for the commercial organoclays are also similar; however, the estimated clay layer charge obtained from the control organoclays shows a higher variation than that observed for the reduced-CEC and commercial organoclays.

The WAXS results obtained for these organoclays are shown in Figure 2. This figure shows that the *d*-spacings for the two-tailed organoclays are significantly higher than those for the one-tailed organoclays. There is a slight decrease in *d*-spacing from the commercial to the control organoclays, and a more noticeable decrease is observed as the CEC is reduced. Furthermore, the intensities of the primary diffraction peaks (d_{001}) are sharper in the control organoclays than those observed for the commercial organoclays; the removal of excess surfactant in the control organoclay may produce higher homogeneity in the layer spacings and increased peak intensity. Figure 2 also shows that the peaks from the reduced-CEC organoclays are wider and at lower *d*-spacings than the peaks from the organoclays with no CEC reduction. The *d*-spacings for the organoclays with low charge reduction are close to those obtained for the organoclays with the medium charge reduction, while the *d*-spacings for the organoclays with high charge reduction are noticeably lower.

Paul et al. showed through experimental and molecular dynamics simulation studies that the *d*-spacing increases linearly with the mass ratio of intercalated surfactant to clay as the surfactant structure and the CEC are varied.[34] Figure 3 shows a single linear relationship between the *d*-spacing and the mass ratio of intercalated surfactant to clay for all organoclays prepared in this study independent of the type of organic modifier used. The organoclays made from the two-tailed surfactant occupy the upper portion of this linear relationship while the organoclays made from the one-tailed surfactant form the lower one. For each type of organic modifier, the commercial organoclays are located in the upper part of the linear relationship, followed by the control organoclays. The points representing the organoclays with low and medium CEC reductions fall lower in this linear relationship while the organoclays with the highest CEC reduction are the lowest points in both cases.

The above results show that the amount of organic modifier contained in the clay galleries is larger for the organoclays exchanged with the two-tailed surfactant than for those containing a one-tailed surfactant; this is consistent with the higher molecular weight of the two-tailed organic modifier. In addition, for both types of organoclays, the amount of organic modifier is largest for the commercial organoclays while the control organoclays have a slightly lower amount of organic modifier. The reduced-CEC organoclays have a noticeably lower value that tends to decrease with extent of CEC reduction; this suggests that a reduction in CEC was achieved for the heated clays, and that dif-

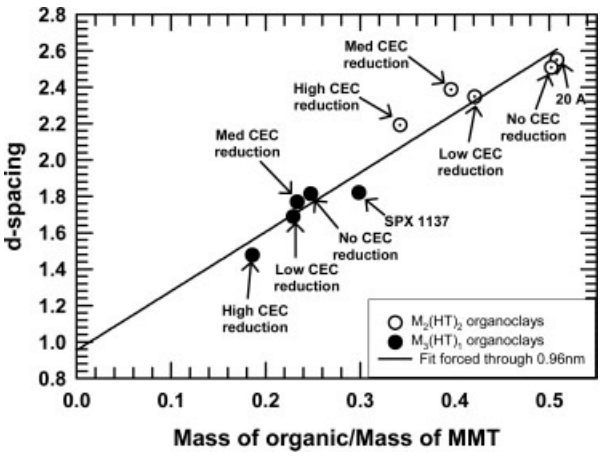

Figure 3 Relationship between organoclay *d*-spacing and mass ratio of intercalated surfactant to clay for the organoclays analyzed in this study.

ferent levels of CEC reduction were obtained. Even though the organoclays with low and medium CEC reductions have very similar organic contents, a clear decrease was observed for the organoclays containing the highest CEC reduction with respect to the control and commercial organoclays. For a specific organic modifier, a lower amount of surfactant in the galleries may be the result of several factors, e.g., a lower reaction yield, the removal of excess surfactant through purification, and/or a reduction in the CEC. The results presented here suggest that the purification procedure performed for the control and reduced-CEC organoclays may be the main factor contributing to the differences observed between the control and commercial organoclays even though other factors like exchange yield or reaction conditions may also have an effect. In the case of the reduced-CEC organoclays the results show an even lower amount of organic modifier, while the broader X-ray diffraction peaks observed for these organoclays also suggest a distribution of gallery spacings from platelet to platelet or along the same platelet (or both) which may stem from heterogeneities in layer charge and charge distribution. In addition, the diffraction peaks from the control organoclays were sharper; this suggests that charge heterogeneity may have been produced by the CEC-reduction process, that is, the charge density may be variable across the breadth of platelets or from platelet to platelet. The differences in morphology and Young's modulus observed for PA-6 and PP/PP-g-MA nanocomposites formed from these organoclays are shown next.

RESULTS AND DISCUSSION

Morphology

Figure 4 shows WAXS scans for the various PA-6 nanocomposites made in this study containing approximately 4.5 wt % MMT, along with the scans of each organoclay for comparison. Figure 4a shows that all the PA-6 nanocomposites containing $M_3(HT)_1$ are absent of any basal reflections, which suggests exfoliated structures. The curves for the nanocomposites made from the control organoclay and the organoclay containing the highest charge reduction show very subtle reflections around 2θ values of 3° and 6°, respectively; the reason for this is not clear at this time, but TEM images shown later confirm the presence of well-exfoliated morphologies in all PA-6/

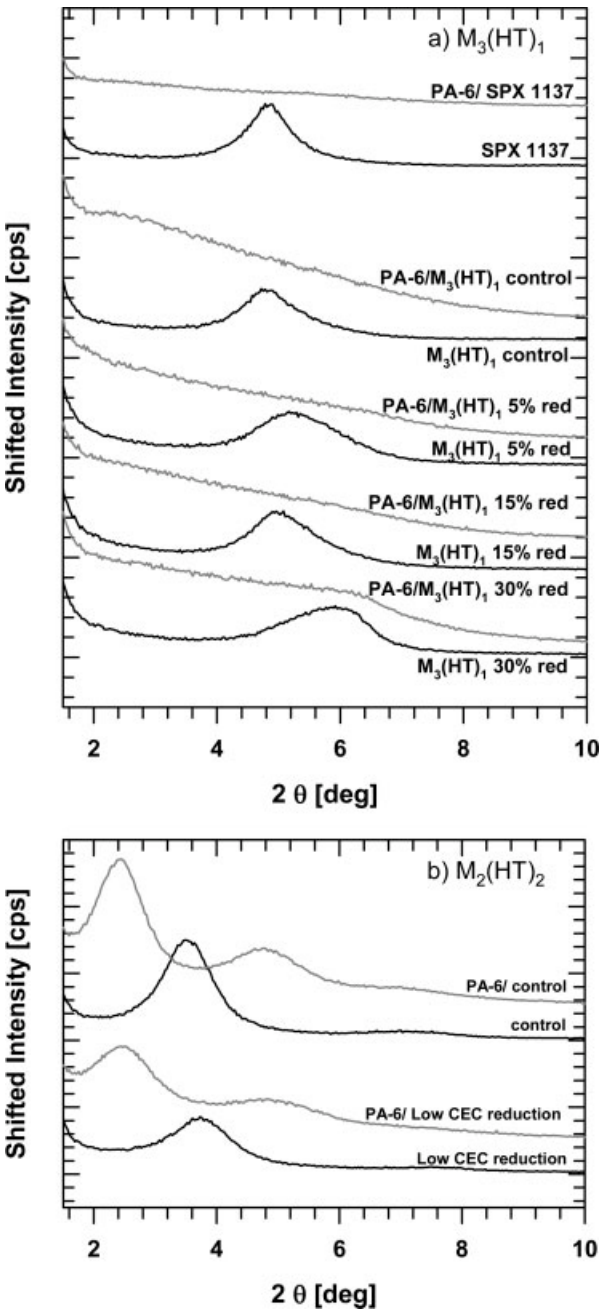

Figure 4 WAXS scans for pure organoclays and their respective PA-6 nanocomposites containing ~ 4.5 wt % MMT.

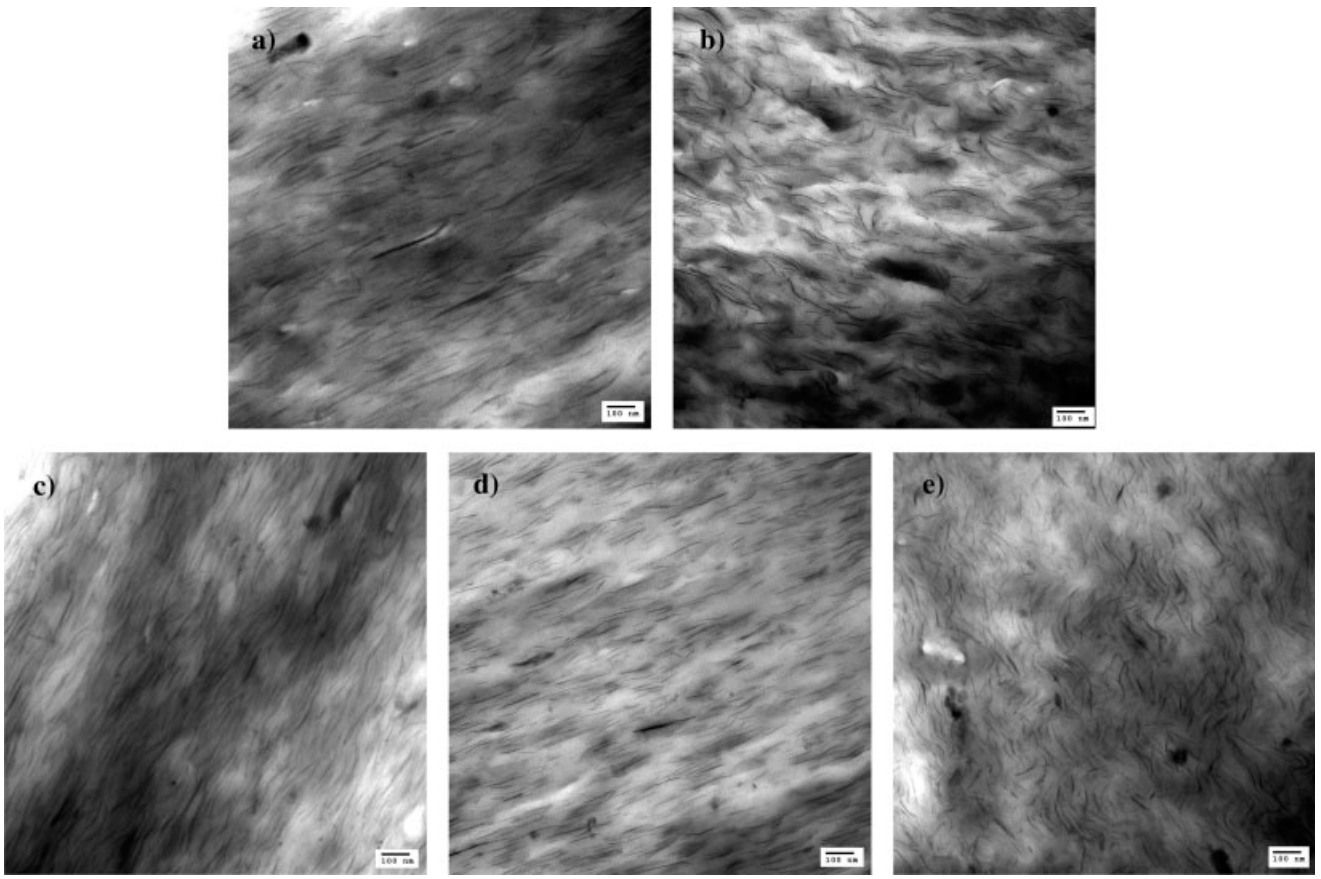

Figure 5 TEM micrographs of PA-6/$M_3(HT)_1$ nanocomposites with high clay concentrations: (a) SPX 1137, (b) $M_3(HT)_1$ control, (c) $M_3(HT)_1$ low CEC reduction, (d) $M_3(HT)_1$ med CEC reduction, and (e) $M_3(HT)_1$ high CEC reduction.

$M_3(HT)_1$ nanocomposites including these two cases. On the other hand, the X-ray scans from select PA-6/$M_2(HT)_2$ nanocomposites shown in Figure 4b have basal reflections, indicating the presence of clay agglomerates; the peaks for these nanocomposites are shifted to higher *d*-spacings than those from the pure organoclays which is consistent with some degree of intercalation into the clay galleries. Figure 4b also shows that the increase in *d*-spacing for both nanocomposites is very similar with respect to their corresponding organoclays.

Figure 5 shows representative TEM micrographs for PA-6/$M_3(HT)_1$ nanocomposites with concentrations of approximately 4.5 wt % MMT. All systems have extremely high levels of exfoliation and no significant differences in particle size or the number of particles that could be observed, except for a small number of slightly larger particles that appear occasionally in the composites made from the reduced-CEC organoclays. TEM micrographs of select PA-6/$M_3(HT)_1$ nanocomposites with concentrations of approximately 1.5 wt % MMT are shown in Figure 6. A higher number of particles with longer lengths is observed for the nanocomposites made from the control organoclay, while the composites made from the commercial organoclay and the organoclay with the highest CEC reduction show a slightly lower number of particles with shorter lengths. Additionally, TEM micrographs of PA-6/$M_2(HT)_2$ nanocomposites with high clay concentrations made from the control organoclay and the organoclay with a low CEC reduction are shown in Figure 7. A significantly lower degree of exfoliation is observed in these nanocomposites with respect to the ones prepared with the one-tailed organoclays, which is consistent with the WAXS results shown above, as well as with previous studies by Fornes et al.[11] The morphologies from the composites shown in this figure are very similar, with slight indications of higher platelet dispersion for the nanocomposite made from the control organoclay.

In the case of PP/PP-*g*-MA nanocomposites, the WAXS scans are shown in Figure 8. All of the samples show basal reflections indicating the presence of large stacks of platelets. The peaks are broader and shifted to lower *d*-spacings than those of the pure organoclays, which suggests a decrease in the interplatelet distance probably from early stages of surfactant degradation during melt processing.[35] TEM images of these nanocomposites are shown in Figures 9 and 10. Figure 9

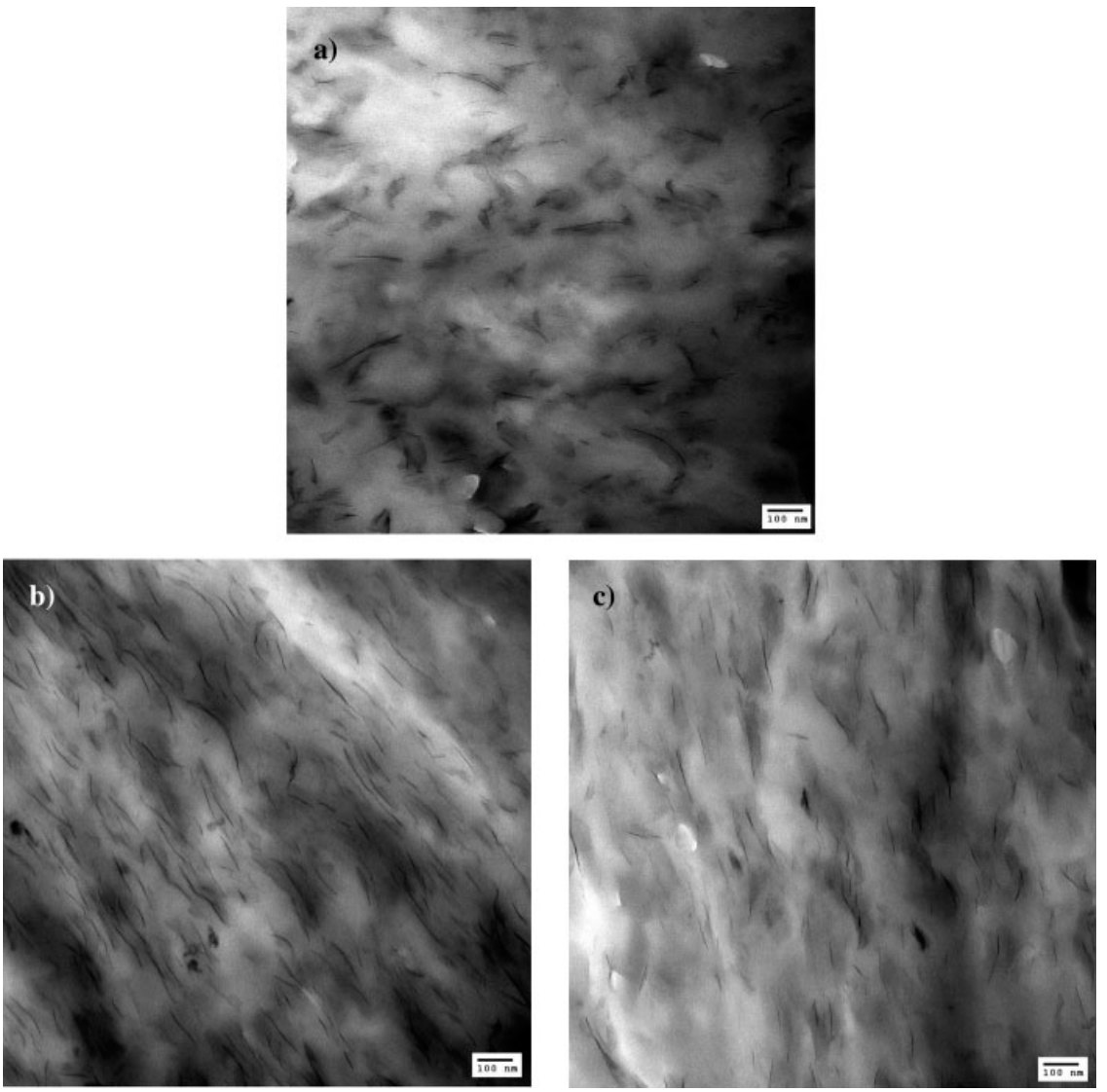

Figure 6 TEM micrographs of PA-6/$M_3(HT)_1$ nanocomposites with low clay concentrations: (a) SPX 1137, (b) $M_3(HT)_1$ control, and (c) $M_3(HT)_1$ high CEC reduction.

shows nanocomposites with concentrations of approximately 4.5 wt % MMT; the nanocomposites made from organoclays with reduced CEC show very large organoclay particles that are not seen in the nanocomposites containing the commercial and control organoclays. When comparing the nanocomposites made from the commercial and the control organoclays, both nanocomposites have fairly small and regular particles; the nanocomposites containing the control organoclay show larger particles, but of considerably smaller sizes than those observed for the composites made from the reduced-CEC organoclays. TEM micrographs of select nanocomposites at lower concentrations (Fig. 10) show a uniform morphology. The nanocomposites containing the commercial organoclay show large particles with high platelet order. Slightly larger, more disordered particles are seen in the samples made from the control organoclay, while the composites made from the organoclay with a high CEC reduction show even larger particles with low platelet order.

Mechanical properties

Figure 11 shows the effect of clay concentration on Young's modulus for the nanocomposites prepared in this study. The modulus increases in all cases as the clay concentration is increased, even at low loadings. For PA-6 nanocomposites, the largest increase in Young's modulus is observed for the composites containing $M_3(HT)_1$ organoclays (Fig. 11a). Here, the control organoclay produces the largest increase in modulus followed by the corresponding commercial organoclay. The organoclays containing low and medium CEC reduction lead to very similar modulus values,

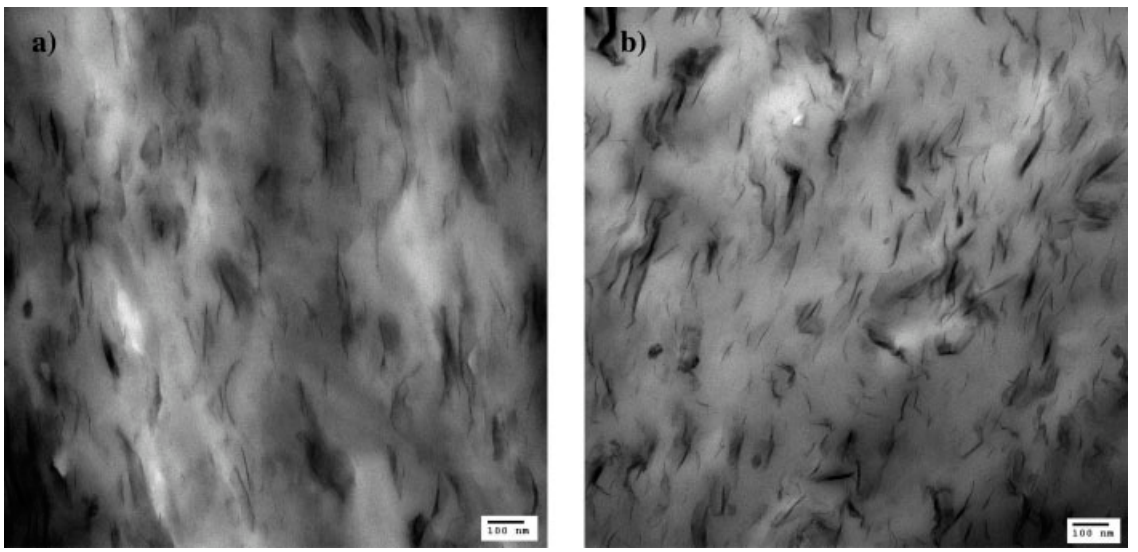

Figure 7 TEM micrographs of PA-6/$M_2(HT)_2$ nanocomposites with high clay concentrations: (a) $M_2(HT)_2$ control and (b) $M_2(HT)_2$ low CEC reduction.

both lower than that of nanocomposites made from the organoclay with the highest CEC reduction. On the other hand, Figure 11b shows that no significant difference was observed in the Young's modulus for PA-6 nanocomposites made from the $M_2(HT)_2$ control organoclay and the corresponding organoclay containing low CEC reduction. Figure 11c shows the modulus of PP/PP-*g*-MA nanocomposites containing the $M_2(HT)_2$ organoclays. The modulus is highest for the composites made from the commercial organoclay, while no significant difference in modulus was observed between the nanocomposites containing the control and reduced-CEC organoclays.

The morphology and modulus results show that PA-6 nanocomposites formed from the one-tailed control organoclay have a higher clay dispersion and modulus enhancement than those containing the corresponding commercial organoclay. Conversely, the two-tailed commercial organoclay produced higher clay dispersion and modulus enhancement for PP/PP-*g*-MA nanocomposites than the corresponding control organoclay. The removal of the small amounts of excess organic modifier may increase the affinity between the PA-6 and the organoclay; at the same time, it may result in a lower hydrophobicity of the organoclay leading to a lower affinity with the nonpolar matrix. On the other hand, the evidence reported here shows that the reduced-CEC organoclays lead to lower exfoliation and modulus enhancement for both PA-6 and PP/PP-*g*-MA nanocomposites; there seems to be no clear correlation with the amount of CEC reduction. We suggest that these observations may not be a definitive assessment of how CEC affects exfoliation in these systems because of some concerns about the uniformity of the CEC reduction. Clearly, the reduced-CEC organoclays contain a lower amount of organic modifier than the organoclays from unmodified clay. The ''macroscopic'' measurements

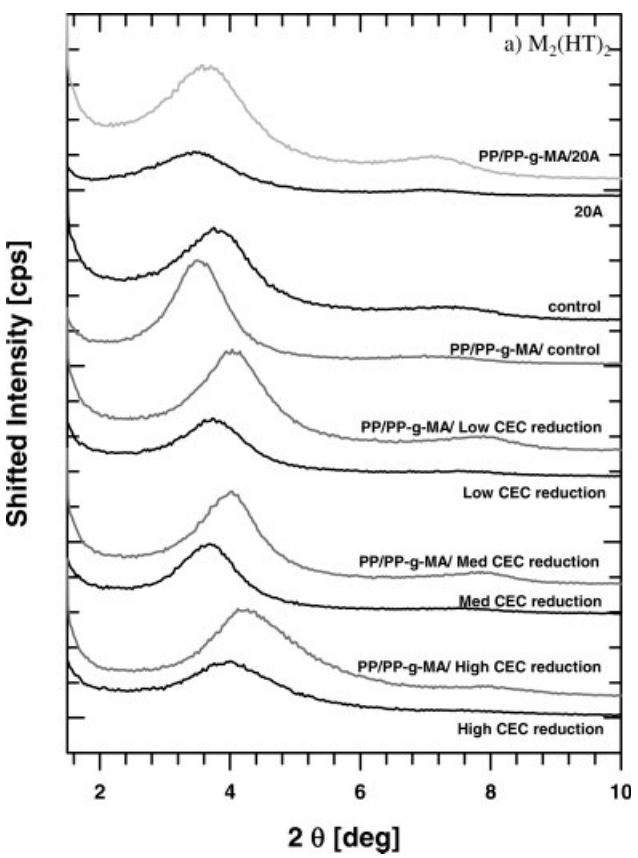

Figure 8 WAXS scans for pure organoclays and their respective PP/PP-*g*-MA/$M_2(HT)_2$ nanocomposites containing ~ 4.5 wt % MMT.

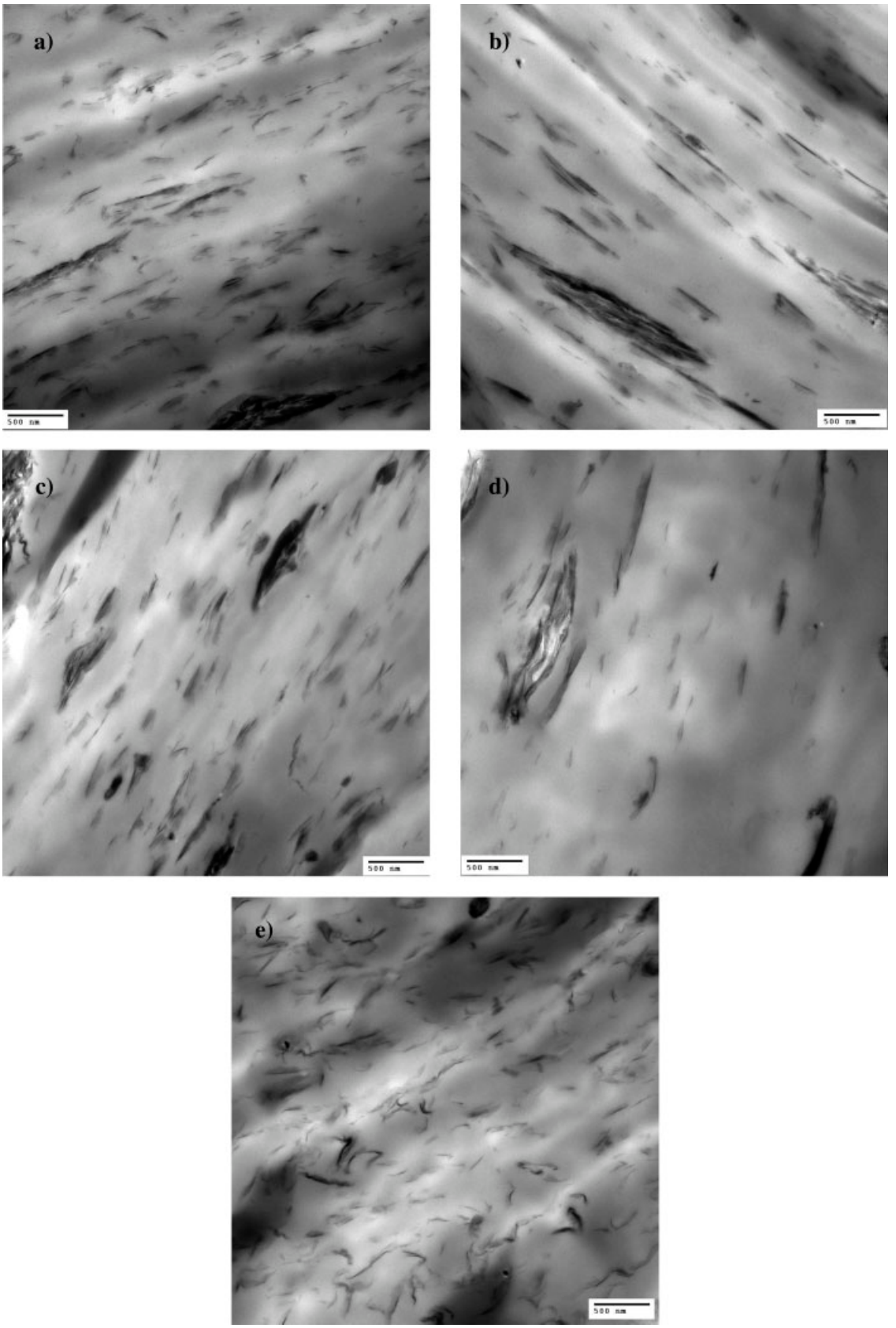

Figure 9 TEM micrographs of PP/PP-*g*-MA/$M_2(HT)_2$ nanocomposites with high clay concentrations: (a) 20A, (b) $M_2(HT)_2$ control, (c) $M_2(HT)_2$ low CEC reduction, (d) $M_2(HT)_2$ med CEC reduction, and (e) $M_2(HT)_2$ high CEC reduction.

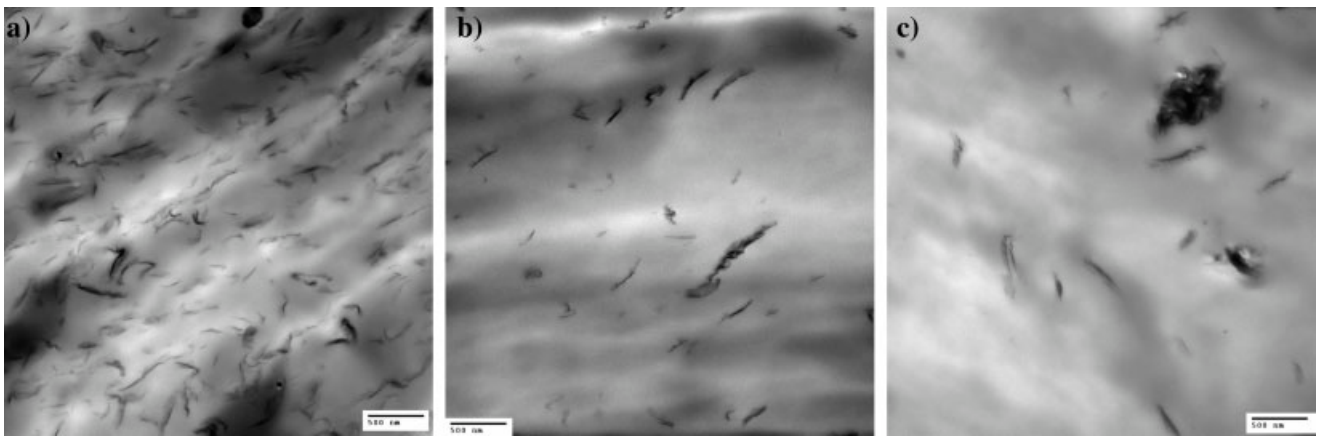

Figure 10 TEM micrographs of PP/PP-*g*-MA/$M_2(HT)_2$ nanocomposites with low clay concentrations: (a) 20A, (b) $M_2(HT)_2$ control, and (c) $M_2(HT)_2$ high CEC reduction.

of CEC and LOI, however, cannot determine the differences in layer charge and charge distribution from gallery to gallery and/or within the same galleries that may be present and that could influence the exfoliation of the organoclay in the polymer matrix. We have no direct measurements at this time to support such variations; however, the breadth of the X-ray diffraction peaks strongly hints at such heterogeneities.

Most of the literature referenced in this study describe a different procedure for CEC reduction of Na-MMT by lithium fixation than the one employed here. That procedure is based on the method reported by Brindley and Ertem[20] and involves mixing Li-MMT and Na-MMT in different proportions depending on the percentage of Li^+ desired, and dispersing the mixture in water.[20] Since Li-MMT and Na-MMT can be completely dispersed in water, an even distribution of Li^+ and Na^+ ions inside the clay galleries can be established before subsequent drying and heating are performed.[20] The kinetic process involved in the adsorption of Li^+ and Na^+ ions in solution into the surface of the clay platelets is assumed to be an equilibrium process where there is no selectivity for Li^+ over Na^+ or *vice versa*; therefore, after eventual ion exchange equilibration there should be equal amounts of Li^+ and Na^+ ions on each platelet. The method for the CEC reduction used here is mainly employed for the CEC reduction of Ca-MMT, since this clay does not expand in water beyond 1.9 nm.[20] It appears that only one other study has been reported using the procedure adopted here,[21] but they describe a more dilute suspension for the Li–Na cation exchange reaction and it was performed under dialytic equilibrium with $NaNO_3$. No problems of clay separation from suspension were mentioned in this reference which suggests that a more dilute suspension might reduce or eliminate the problems described above concerning clay separation from the supernatants. The possible differences between these methods are not known at this point, but the results shown above do confirm that high CEC reduction, as described in the other references, could not be achieved through this method.

CONCLUSIONS

Structure–property relationships for PA-6 and PP/PP-*g*-MA nanocomposites prepared by melt processing from a series of reduced-CEC organoclays are presented here. Three reduced-CEC MMT clays were formed from a cation exchange reaction between Na-MMT and LiCl. Since CEC measurements on the as-received clays showed only a minor CEC reduction, subsequent heating based on preliminary tests was performed to target three different levels of CEC reduction, a low, an intermediate, and a high CEC reduction. Two different types of organoclays were produced containing $M_3(HT)_1$ and $M_2(HT)_2$ organic modifiers, along with controls for each type of organoclay made from Na-MMT for comparison. Purifications with methanol were performed for these organoclays to remove the excess surfactant in the clay galleries that could be present from the cation exchange reaction with the alkyl ammonium surfactants. X-ray analysis and LOI calculations for these organoclays showed a reduction in the intergallery spacing and in the amount of organic modifier contained in the clay with increasing levels of CEC reduction. A lower intergallery spacing and amount of organic modifier was also observed for the control organoclays after purification with respect to the corresponding commercial organoclays.

The morphology and modulus results show that the reduced-CEC organoclays formed in this study lead to a lower degree of exfoliation and modulus enhancement for both PA-6 and PP/PP-*g*-MA nanocomposites, even though there seems to be no clear correla-

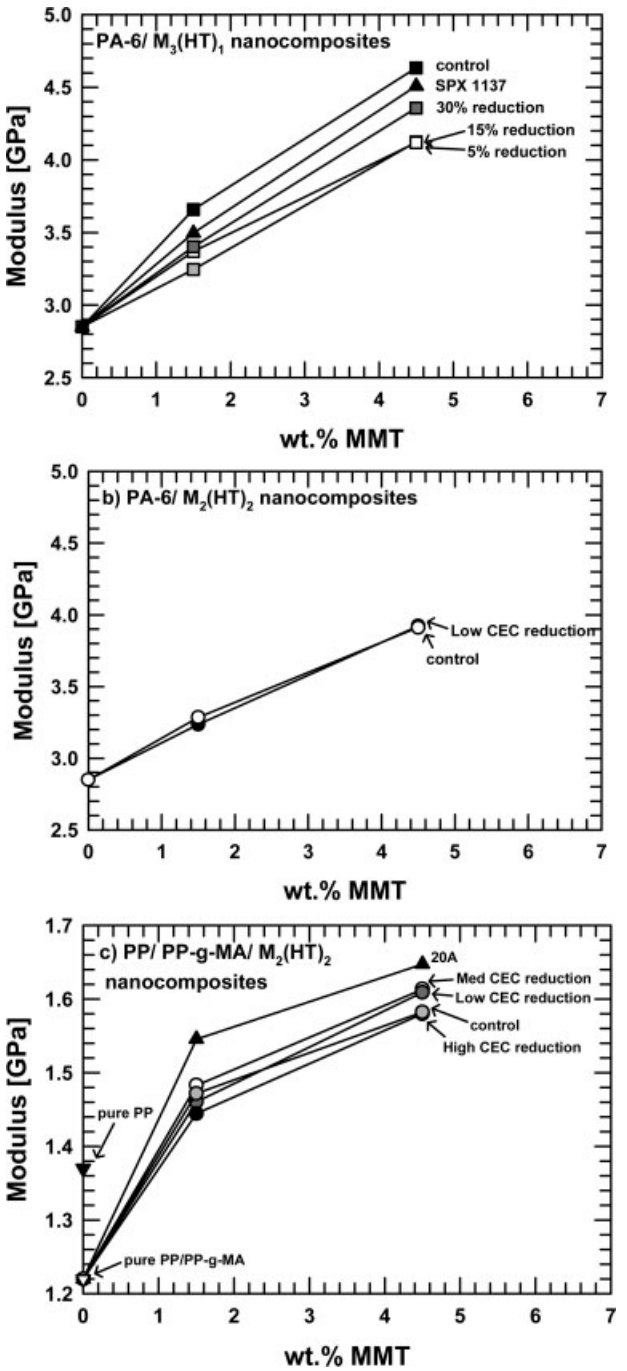

Figure 11 Young's modulus for PA-6 and PP/PP-*g*-MA nanocomposites.

tion with the amount of CEC reduction. These results may be influenced to some degree by differences in layer charge and charge distribution that may have been produced during the charge reduction process. The control organoclay containing the one-tailed surfactant leads to a higher clay dispersion and modulus enhancement of PA-6 nanocomposites than the commercial organoclay, while the two-tailed commercial organoclay leads to higher clay dispersion and modulus enhancement in the case of PP/PP-g-MA nanocomposites. Eliminating any excess organic surfactant in organoclays with no CEC reduction may increase the affinity with PA-6 while this may decrease the affinity with a nonpolar matrix.

More work will be needed to fully assess the effects of CEC on exfoliation, since questions regarding the CEC reduction process and charge heterogeneity could not be fully resolved in this preliminary study. In addition, the small amounts of charge-reduced clay obtained from the current CEC-reduction process limited the extent of clay and nanocomposite characterization.

These preliminary observations on the CEC reduction process give important insights for future work on this subject. A more detailed study revisiting the CEC reduction process and subsequent characterization of the resulting clays should be carried out using the methodologies suggested earlier.

The authors thank Ben Knesek, Joe Ortiz, and Tony Gonzalez from Southern Clay Products Inc. for performing the CEC measurements, WAXS analyses, their assistance in the formation of organoclays, and for many helpful discussions. We would also like to thank Dr. Terry Turney, Director of CSIRO's Nanotechnology Center for proposing and supporting this research.

References

1. Liu, L.; Qi, Z.; Zhu, X. J Appl Polym Sci 1999, 71, 1133.
2. Wang, Z.; Pinnavaia, T. J. Chem Mater 1998, 10, 3769.
3. Hu, Y.; Wang, S.; Ling, Z.; Zhuang, Y.; Chen, Z.; Fan, W. Macromol Mater Eng 2003, 288, 272.
4. Schmidt, D.; Shah, D.; Giannelis, E. P. Curr Opin Solid State Mater Sci 2002, 6, 205.
5. Yano, K.; Usuki, A.; Okada, A.; Kurauchi, T.; Kamigaito, O. J Polym Sci Part A: Polym Chem 1993, 31, 2493.
6. Messersmith, P. B.; Giannelis, E. P. J Polym Sci Part A: Polym Chem 1995, 33, 1047.
7. Chen, W.; Xu, Q.; Yuan, R. Z. Mater Sci Eng B: Solid-State Mater Adv Technol B 2000, 77, 15.
8. Chen, W.; Xu, Q.; Yuan, R. Z. Compos Sci Technol 2001, 61, 935.
9. Yoon, P. J.; Fornes, T. D.; Paul, D. R. Polymer 2002, 43, 6727.
10. Dennis, H. R.; Hunter, D. L.; Chang, D.; Kim, S.; White, J. L.; Cho, J. W.; Paul, D. R. Polymer 2001, 42, 9513.
11. Fornes, T. D.; Yoon, P. J.; Hunter, D. L.; Keskkula, H.; Paul, D. R. Polymer 2002, 43, 5915.
12. Lee, H. S.; Fasulo, P. D.; Rodgers, W. R.; Paul, D. R. Polymer 2005, 46, 11673.
13. Shah, R. K.; Hunter, D. L.; Paul, D. R. Polymer 2005, 46, 2646.
14. Komadel, P.; Madejova, J.; Bujdak, J. Clays Clay Miner 2005, 53, 313.
15. Hoffman, U.; Klemen, R. Z anorganische allegemeine Chemie 1950, 262, 95.
16. Calvet, R.; Prost, R. Clays Clay Miner 1971, 19, 175.
17. Bujdak, J; Slosiarikova, H.; Cicel, B. J Inclusion Phenom Molec Recognit Chem 1992, 13, 321.
18. Komadel, P.; Hrobarikova, J.; Smrcok, L.; Koppelhuber-Bitschnau, B. Clay Miner 2002, 37, 543.
19. Hrobarikova, J; Madejova, J; Komadel, P. J Mater Chem 2001, 11, 1452.

20. Brindley, G. W.; Ertem, G. Clays Clay Miner 1971, 19, 399.
21. Maes, A.; Stul, M. S.; Cremers, A. Clays Clay Miner 1979, 27, 387.
22. Meier, L. P.; Nuesch, R. J Colloid Interf Sci 1999, 217, 77.
23. Clemenz, D. M.; Mortland, M. M. Clays Clay Miner 1974, 22, 223.
24. Lagaly, G. Clays Clay Miner 1979, 27, 1.
25. Stul, M. S.; Mortier, W. J. Clays Clay Miner 1974, 22, 391.
26. Delozier, D. M.; Orwoll, R. A.; Cahoon, J. F.; Ladislaw, J. S.; Smith J. G., Jr.; Connell, J. W. Polymer 2003, 44, 2231.
27. Fornes, T. D.; Yoon, P. J.; Keskkula, H.; Paul, D. R. Polymer 2001, 42, 9929.
28. Kim, D. H.; Fasulo, P. D.; Rodgers, W. R.; Paul, D. R. In preparation.
29. Chavarria, F.; Shah, R. K.; Paul, D. R. In preparation.
30. Van Olphen, H. In An Introduction to Clay Colloid Chemistry: For Clay Technologists, Geologists, and Soil Scientists; Wiley: New York, 1977; Chapter 5.
31. Stretz, H. A. Ph.D. Thesis, The University of Texas at Austin, 2005.
32. Greene-Kelly, R. J Soil Sci 1953, 4, 233.
33. Xie, W.; Gao, Z.; Pan, W. P.; Hunter, D. L.; Singh, A.; Vaia, R. A. Chem Mater 2001, 13, 2979.
34. Paul, D. R.; Zeng, Q. H.; Yu, A. B.; Lu, G. Q. J Colloid Interf Sci 2005, 292, 462.
35. Shah, R. K.; Paul, D. R. Polymer 2006, 47, 4075.